



Non-Hermitian elastodynamics in gyro-odd continuum media

Penglin Gao ^{1,2,3}, Yegao Qu^{1,2}✉ & Johan Christensen ³✉

Linear elasticity has long been considered a well-established research area using conservative field theory. However, the discovery of odd-elasticity challenges the essential energy conservation assumption, which together with gyroscopic ingredients compromise the fundamental theory of elasticity, but to the same effect, enable new directions in active elastodynamics. Here, we consider two-dimensional continuum mechanics in a more general framework containing active constituents from both gyroscopic and odd-elastic effects, which gives rise to non-reciprocal and non-Hermitian elastic waves in a highly unconventional guise. We discuss how these unusual media can extract energy from odd-elastic engine cycles comprising remarkable features of stability transitions, in which the energy exchange process reverses. Beyond bulk waves, akin to the unidirectional characteristics of a 2D quantum-Hall insulator, we demonstrate the existence of non-Hermitian Rayleigh surface waves which, in contrast to the classical ones in passive solids, display one-way and interference-free transport characteristics, which even remain resilient in finite sharp or curved geometries. The findings reported here may provide new possibilities to manipulate elastic waves in unusual ways.

¹State Key Laboratory of Mechanical System and Vibration, School of Mechanical Engineering, Shanghai Jiao Tong University, 200240 Shanghai, China. ²Institute of Vibration, Shock and Noise, Shanghai Jiao Tong University, 200240 Shanghai, China. ³Department of Physics, Universidad Carlos III de Madrid, Leganés, Madrid ES-28916, Spain. ✉email: quyegao@sjtu.edu.cn; johan.christensen@uc3m.es

The theory of linear elasticity has long been considered a well-understood area in classical continuum mechanics, however, the booming field of artificial metamaterials offers plenty of different avenues and perspectives to reexamine the basics¹. The directions cover a broad variety of topics ranging from Cosserat elasticity^{2–4}, Willis metamaterial^{5–7}, pentamode metafluid^{8–10} to topological mechanics^{11–14}, just to name a few. Beyond passive media, lately a growing frontier emerged relying on active systems using external bias for various demands such as phononic gain, reconfigurability, or deterministic functionality^{15,16}. Moreover, active metamaterials and artificial lattices have lately also found important use in non-Hermitian, non-reciprocal and even topological physics. Electrically biased piezophononic media^{17–20}, spinning gyroscope networks²¹, spatiotemporal metamaterials^{15,22} and robotic toy models^{23,24}, all are paradigm examples where active bias provides a rich playground for highly unusual wave phenomena and applications with the likes of unidirectional transmission, skin effect, and delocalized topological states, etc. At a more fundamental level, basic symmetry principles that were disregarded in the past, have recently emerged as an intensively investigated branch of active mechanics. One example is the breaking of the time-reversal symmetry using lattices of spinning gyroscopes that is caused by directional dependent inertial forces^{25–28}. In addition, the Maxwell-Betti reciprocity²⁹, a fundamental relation connecting two sets of stress and strain fields, broadly speaking, can be considered as the symmetry between excitation and response. Recently, Scheibner et al.³⁰ discussed the failure of this basic symmetry and the odd wave dynamics in over-damped systems when energy conservation assumption was discarded, giving rise to a loss of major symmetry of the elastic tensor, i.e., $C_{ijkl} \neq C_{klij}$. Such novel odd-elastic material acquires antisymmetric moduli $C_{ijkl}^o = (C_{ijkl} - C_{klij})/2$ from unconventionally introduced non-conservative internal forces powered by internal activity. Thus, the breaking of the two symmetries has significantly broadened the foundation of possibilities in classical elasticity^{27,31–33}, yet it remains to be reported, beyond the over-damped simplification, what implications gyro-odd coupling has for wave propagation in general elastodynamic systems with inertial terms.

In this work, we explore non-Hermitian wave dynamics in 2D elastic media including active ingredients from both the gyroscopic and odd-elastic effects. The creation of active media usually relies on microscopic lattices comprising power-driven

building blocks, which will be treated in the effective continuum limit^{27,30} that permits us to acquire yet unseen elastodynamic wave physics, such as non-Hermitian stability transitions due to odd-elastic energy exchange in unbound media. For the semi-infinite counterpart comprising both gyroscopic and odd-elastic components, we unveil highly resistant non-topological Rayleigh surface waves which, phenomenologically speaking, display features reminiscent to chiral edge states in topological Chern insulators. Hence, the non-Hermitian gyro-odd-elastic Rayleigh waves confine along the interface in one direction and are capable to propagate around sharp corners and bends with largely suppressed parasitic scattering interference. Moreover, we display how these designer Rayleigh waves can be engineered with arbitrary propagation and penetration lengths. Generally speaking, we emphasize that gyro-odd coupling leads to highly unusual elastodynamic features that are unattainable in purely gyroscopic or over-damped odd-elastic systems.

Results and discussion

Continuum gyro-odd-elasticity. A gyro-odd-elastic lattice is schematically illustrated in Fig. 1a, which displays a triangular arrangement of lumped masses that are mounted on spinning gyroscopes and connected to the six nearest neighbors through active bonds. The former introduces gyroscopic coupling, whereas the latter generates non-conservative interactions. The active bonds, as shown in the inset of Fig. 1a, when perturbed through elongation or contraction, produce not only axial restoring forces F_r , but also transverse forces F_ψ , which deviate from the conservative force law of the standard Hookean springs³⁰. Under small perturbations, this network permits movement only in the lattice plane $O(x_1, x_2)$. Thus, in the strict long wavelength regime, we can reasonably well treat the gyro-odd-lattice as a 2D continuum metamaterial^{27,30,32}. Specifically, the inertial forces arising from the gyroscopic effect can be effectively mapped into a density tensor^{21,27}

$$\rho = \begin{pmatrix} \rho & i\alpha \\ -i\alpha & \rho \end{pmatrix}, \quad (1)$$

where ρ is the inertial density, and α reflects the level of gyricity. We emphasize that the imaginary unit in the off-diagonal terms, expresses the phase delay between the gyroscopic force and

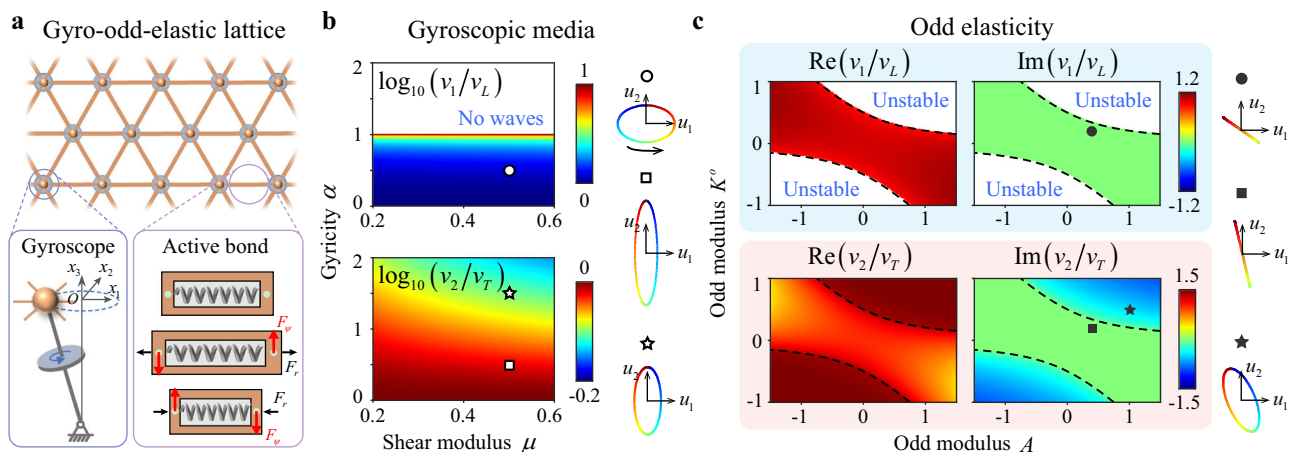


Fig. 1 Active lattice comprising gyroscopic and odd-elastic effects. **a** A lattice model illustrating how to introduce the two active ingredients: the lumped masses are mounted on spinning gyroscopes to harness gyroscopic coupling. Active bonds that can generate non-conservative forces fuel the odd-elastic response. **b** Phase diagrams for the two branches of waves in purely gyroscopic media ($A = K^o = 0$). The colored regions depict the phase velocities v_1 and v_2 . Several points are chosen to show the polarization trajectories, moving from blue to red. **c** Likewise in **b**, but now depicting the complex velocities for purely odd elasticity when $\mu = 0.5$ and $\alpha = 0$. In this figure, the blank regions indicate either the absence of waves or mechanical instability. The velocities v_1/v_2 are normalized with their counterparts in passive solids v_L/v_T , with the subscript denoting the longitudinal (L) or transverse (T) waves.

displacement, but has no additional influence on the energy dissipation. The stress-strain relationship for the active bonds, despite the non-conservative force law in the continuum limit, is ordinarily expressed through the generalized Hooke's law $\sigma_{ij} = C_{ijkl}u_{l,k}$ which for convenience is reformulated in matrix notation as $\sigma^\alpha = C^{\alpha\beta}s^\beta$ where α and β take integer values from 0 to 3 (see Supplementary Note 1 for details). Here, σ^α and s^β are the decomposed components of the stress tensor σ_{ij} and the displacement gradient tensor $u_{l,k} = \partial u_l / \partial x_k$, respectively. We focus here on 2D isotropic solids whose less ordinary stiffness matrix reads³⁰

$$C = 2 \begin{pmatrix} B & 0 & 0 & 0 \\ A & 0 & 0 & 0 \\ 0 & 0 & \mu & K^o \\ 0 & 0 & -K^o & \mu \end{pmatrix}. \quad (2)$$

Beyond the familiar bulk B and shear modulus μ , the stiffness matrix is now attributed by two odd-elastic moduli A and K^o . Based on the continuum descriptions, the equation of motion is given by

$$\left(C_{ijkl}u_{l,k} \right)_{,i} = \rho_j \ddot{u}_i, \quad (3)$$

which sustains time-harmonic solutions in unbound space, i.e., $\mathbf{u} = \tilde{\mathbf{u}}e^{i(\mathbf{k}\cdot\mathbf{x} - \omega t)}$. Here, $\tilde{\mathbf{u}}$ denotes the complex amplitude of the displacement, \mathbf{k} and ω are, respectively, the wave vector and angular frequency. The substitution of harmonic solutions into Eq. (3) yields the dispersion relation of non-Hermitian elastic waves (see Supplementary Note 2), detailed theoretical analyses reveal that, when $|\alpha/\rho| < 1$ there are two branches of non-dispersive waves having phase velocities v_1 and v_2 , which in the passive limit correspond to the longitudinal ($v_1 = v_L$) and transverse waves ($v_2 = v_T$), respectively. By contrast, when $|\alpha/\rho| \geq 1$ only one pseudo-transverse branch remains, while the other one related to v_1 vanishes due to the strong gyroscopic effect.

To shed some light on the role of the two ingredients, we consider two scenarios sustaining either gyroscopic (Fig. 1b) or odd-elastic effects (Fig. 1c) separately. All the material properties are dimensionless by setting $\rho = 1$ and $B = 1$. Figure 1b, c depict v_1 and v_2 in the gyro-odd-parameters space, from which the general wave dynamics can be unveiled. In Fig. 1b, what clearly stands out is a transition boundary that divides the (μ, α) plane into subcritical ($\alpha < 1$) and supercritical ($\alpha > 1$) regions. With growing gyricity α , it is seen that v_1 grows rapidly until the critical point ($\alpha = 1$) above which it ceases to exist. On the other hand, with growing gyricity v_2 gets smaller and displays no signs of a transition. Since the gyroscopic forces tend to move segments of the material in elliptical orbits, we observe that the two branches exhibit hybridized polarization patterns as illustrated in Fig. 1b, comprising either longitudinal- (for v_1 , circle) or transverse-dominated (for v_2 , star and square in the (μ, α) plane) motions, which will not happen in conventional isotropic solids. For odd-elasticity, Fig. 1c displays completely different characteristics in comparison to the gyroscopic media. First, complex velocities are obtained since the odd-elastic effect drives the dispersion relation to be fully complex. Mechanical stability requires $\text{Im}(v_{1,2}) \leq 0$ (color region), otherwise $\text{Im}(v_{1,2}) > 0$ (blank region), corresponding to amplified vibrational modes, which implies a collapse of the solid structure owing to the growing energy injection in the material bulk. Second, as shown by the polarization charts, the eigenvectors experience an abnormal transition from linear to elliptical polarization that is separated by the activity threshold $K^o(A + K^o) = (B/2)^2$ (dashed lines). Interestingly, the eigenvectors become co-linear at this transition boundary, which is a hallmark feature of exceptional points and marks the onset of

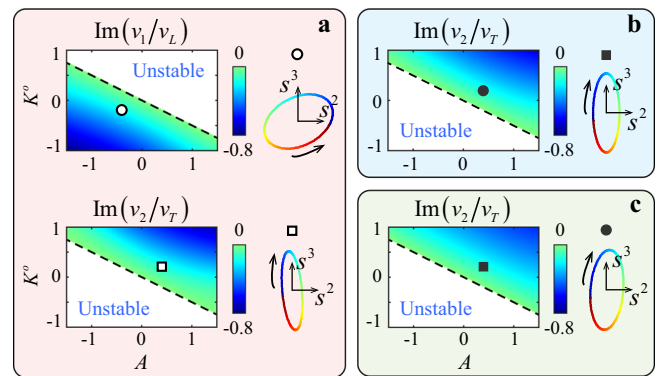


Fig. 2 Gyro-odd elastodynamics in unbound media. **a** Phase diagrams showing the stability transition in the odd-elastic parameters space. The other material properties are chosen as $\mu = 0.5$ and $\alpha = 0.5$. The dashed lines mark the transition boundary, that is $A + 2K^o = 0$. The colored (stable) regions depict the imaginary parts of $v_{1,2}$. As indicated by the symbols, some odd-elastic engine cycles are provided in the strain subspace (s^2, s^3) to analyze the mechanical work done on the solid. Likewise, **(b, c)** present the results for the cases $\alpha = 1$ and $\alpha = 2$, respectively, but now only the v_2 branch exists.

non-Hermitian elastodynamics. In terms of energy exchange, this non-Hermitian spectral singularity signifies the onset of nonzero work generated by the non-conservative active force, which happens when it starts to drive a material segment to form a closed engine cycle. Below the activity threshold, the odd-elastic moduli will not induce non-Hermitian features because the active forces are not sufficiently strong to drive particles to form closed engine cycles. Above it, however, the complex velocities indicate either attenuated or unstable solutions due to the nonzero energy extracted from the odd-elastic engine.

The complete elastodynamics comprising both odd-elasticity and gyro-activity as expressed in equation (3) enriches the entire wave scenario. While the threshold $\alpha = 1$ of the gyricity level at which one branch of the solutions ceases to exist prevails, the combined gyro-odd stability transition borders at $A + 2K^o = 0$ as seen in Fig. 2 (see Supplementary Note 2). In this figure, $\text{Im}(v_{1,2})$ is depicted for three typical gyroscopic cases: (a) $\alpha = 0.5$; (b) $\alpha = 1$; and (c) $\alpha = 2$. In comparison to Fig. 1c, here the velocities acquire imaginary parts for any odd-elastic parameters (A, K^o) except for $A = -2K^o$ (the dashed lines). We ascribe this to the gyroscopic effect, because it drives a medium segment moving along an elliptical trajectory, whose engine cycle persists for any odd-elastic material properties, giving rise to gain or loss of elastic energy through mechanical work:

$$W = (A + 2K^o)S_h, \quad (4)$$

where S_h is the area enclosed by a path in strain subspace $\mathbf{h} = (s^2, s^3)$ (see Supplementary Note 4). In detail, the quantity W , defined as the work done on the solid per unit area, measures the energy injected in ($W > 0$, unstable) the material or flowing outward ($W < 0$, stable) during one odd-elastic engine cycle. Hence, the sign of W determines the stability of odd elasticity. At the gyro-odd stability transition ($A = -2K^o$), the mechanical work cancels out, $W = 0$ [Eq. (4)], which is clearly seen in the odd-elastic (A, K^o) phase-maps shown in Fig. 2. In addition, some representative engine cycles are displayed to clarify the mechanical work for some selected points. All four cases, according to equation (4), produce negative work $W < 0$, which explains the loss of elastic energy as indicated by the velocities of negative imaginary parts $\text{Im}(v_{1,2}) < 0$.

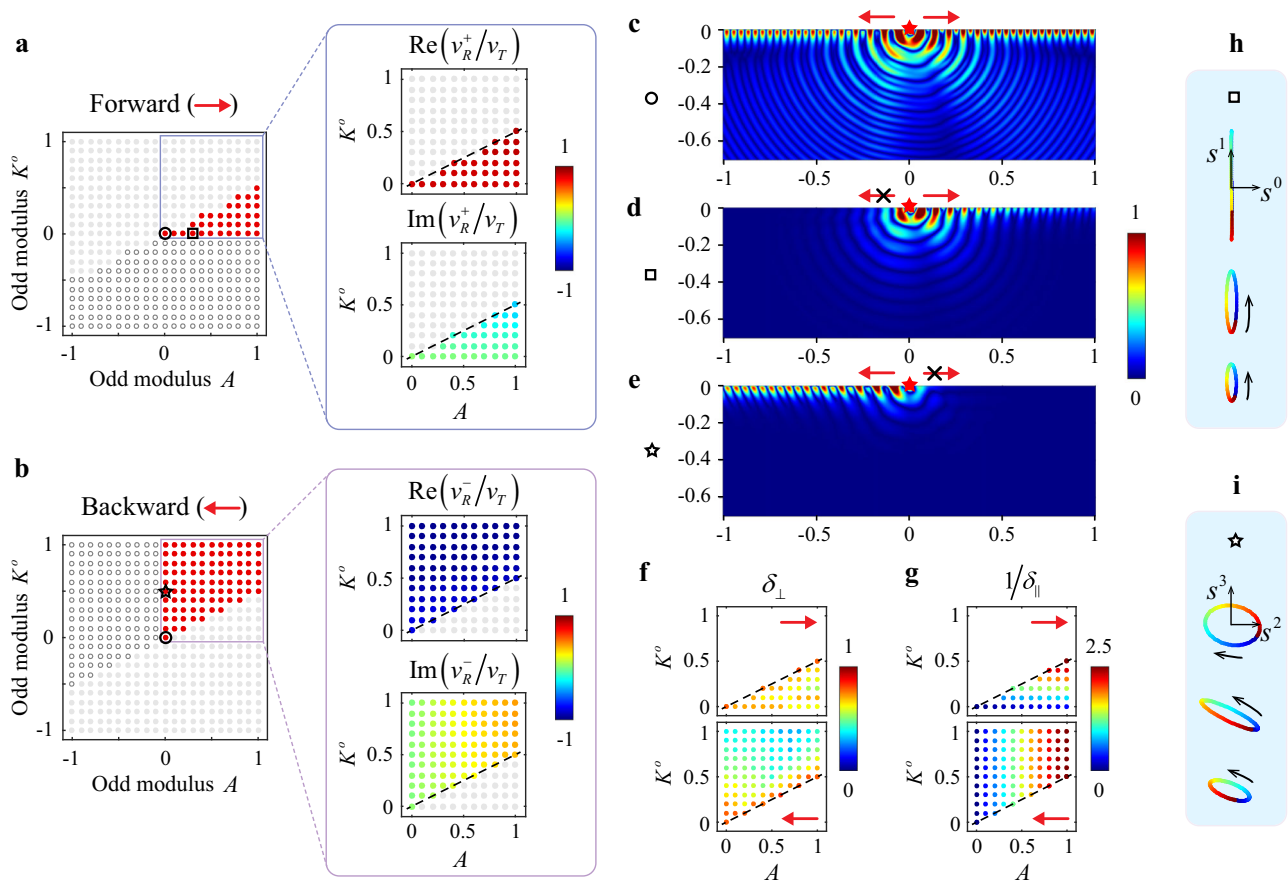


Fig. 3 Non-Hermitian Rayleigh waves in half-space. **a** Scatter plots showing the phase diagram and the complex velocity v_R^+ for the forward propagating Rayleigh waves, and **b** corresponding to v_R^- in the backward direction. Beyond the stable solutions (red dots), we use gray dots and hollow circles to differentiate between no solution and instability, respectively. The red arrows indicate either a forward or backward propagating direction. The dashed lines mark the transition of one-way propagation reversal. **c–e** Numerically calculated modal fields with parameters highlighted in **(a, b)**. In each simulation, a vibrating source (red stars, $\omega = 15\pi$) is placed on the top surface to excite surface waves, and the modal fields are normalized with regard to their own maximum values. **f, g** Scatter maps rendering the penetration depth δ_{\perp} and the reciprocal propagation length $1/\delta_{\parallel}$ (normalized to the wavelength) for the non-Hermitian Rayleigh waves. In here, we discriminate between forward and backward propagating waves. **h** A group of odd-elastic engine cycles at different depths for the Rayleigh waves studied in **d**. **i** Likewise for the scenario illustrated in **e**. In this study, we set material parameters $\mu = 0.5$ and $\alpha = 1$.

Non-Hermitian Rayleigh waves. Conventional Rayleigh waves are surface bound waves comprising elliptical segment motion. Adding gyro-odd elasticity to a half-space as seen in Fig. 3 should provide a non-Hermitian and non-reciprocal propagation channel with energy exchange between the artificial solid and its surrounding. By formulating a directional Ansatz solution for non-Hermitian Rayleigh waves, we obtain complex forward (backward) Rayleigh velocities v_R^+ (v_R^-) as depicted by the scatter plots shown in Fig. 3a (Fig. 3b) (see Supplementary Notes 3 and 5 for details). In the scatter diagrams, the gray dots indicate the absence of surface waves, while the red dots and the hollow circles mark stable and unstable solutions, respectively. We note that surface waves appear only if the odd-elastic moduli are all non-negative (highlighted quadrants in Fig. 3a, b). In this zone, a unidirectional transition threshold features the odd-parameter space, which indicates that fully rectified Rayleigh surface waves can flip their one-way path beyond this border. We place a point source at the half-space interface to probe various phases in the odd-parameter space. At its origin, i.e., the circle in Fig. 3a, b, gyroscopic coupling only prevails by virtue of weak asymmetric Rayleigh wave spreading, however, at the cost of visible vibrational bulk penetration as shown in Fig. 3c. In stark contrast, once odd-elasticity is included (star and square in Fig. 3a, b) the

non-Hermitian Rayleigh waves display a highly non-reciprocal response to the excitation source, where in fact, both the one-sided propagation length δ_{\parallel} and the penetration depth δ_{\perp} can be designed at will as shown in Fig. 3d, e. To elaborate on this, we compute those two quantities, which are defined as length scales at which the displacement amplitude decays to $1/e$ along their respective directions. The map of δ_{\perp} (Fig. 3f), similar to passive media, shows a strong confinement of Rayleigh waves at the order of one wavelength. Regarding the propagation length as shown in Fig. 3g, we predict a tunable response in dependence of the odd-elastic moduli, ranging from nearly infinite to merely several wavelengths. Thus, the entire odd-elastic parameter space, elegantly displays how surface vibrations can be tailored for long- or short-range propagation. Upon closer inspection of the mechanical work done by the non-Hermitian Rayleigh waves: $W = \int_{-\infty}^0 [-AS_g(x_2) + 2K^o S_h(x_2)] dx_2$, where S_g and S_h are the enclosed areas in the strain subspaces $\mathbf{g} = (s^0, s^1)$ and $\mathbf{h} = (s^2, s^3)$, respectively (see Supplementary Note 4), we display the shallow depth engine cycles of the two one-way surface waves as shown in Fig. 3h, i. Both scenarios produce negative net work, however, the reversion of the cycle as seen in Fig. 3i compensates loss of elastic energy, which consequently enables extended propagation lengths as shown in Fig. 3e.

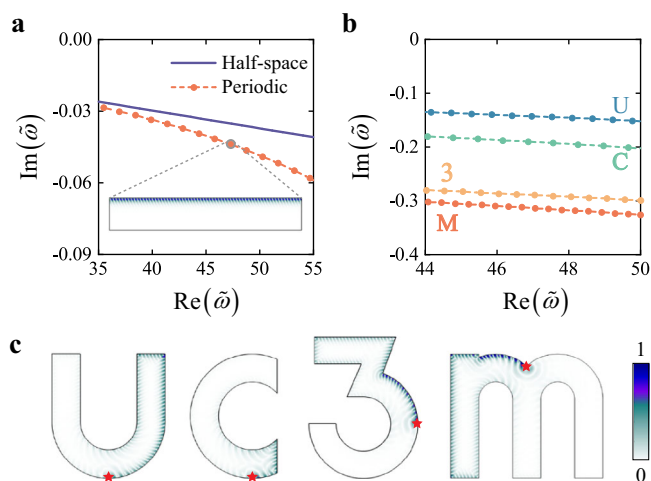


Fig. 4 Rayleigh waves in bound media. **a** Calculated eigenfrequencies $\tilde{\omega}$ (dots) of a finite slab with periodic boundary conditions in the horizontal directions compared to the theoretical solution (solid line) of a half-space. Inset: one representative Bloch wavefield at the selected point. **b** Eigenfrequencies of individual letters (numerically calculated), i.e., "UC3M" as depicted below. **c** Simulated displacement fields when the letters are excited by local vibrations (red stars, $\omega = 15\pi$). In the calculation, the parameters are specified as $\alpha = 1$, $\mu = 0.5$, $A = 0$, and $K^o = 0.5$, and the wavefields are normalized with regard to their own maximum values.

Non-topological elastic resilience. While non-Hermiticity and non-reciprocity jointly have displayed unusual non-Bloch bulk-boundary properties in terms of topological skin effects^{19,34}, we show in the following that the energy exchange assisted by gyro-odd-elasticity as well leads to wave characteristics that are impossible to be captured by Bloch's theorem. We take a sufficiently sized gyro-odd slab (see the inset of Fig. 4a) and apply periodic boundary conditions to mimic a half-space. The complex eigenfrequencies of non-Hermitian Rayleigh waves are plotted in comparison to the theoretical predictions of such half-space as shown in Fig. 4a. Based on the non-reciprocity and energy-exchange induced wave attenuation, we predict that the Bloch-wave based solution diverges from the analytical prediction. The result thereof is clearly seen in Fig. 3e, where the gyro-odd Rayleigh waves exhibit rather distinctive features in comparison to the periodic Bloch wavefield (inset of Fig. 4a), suggesting that one-way lossy properties have no periodic solutions. However, the fact that those complex waves only vibrate in one direction, raises the question as to whether features of a Chern insulator^{25,26,35} can be found in gyro-odd continuum media in the absence of a band topology. Thus, we excite non-Hermitian Rayleigh waves in geometrical shapes of letters to argue whether parasitic scattering is formed. Despite the lossy channels as captured by the complex eigenvalues in Fig. 4b which provides finite propagation, we clearly see in Fig. 4c that the gyro-odd Rayleigh waves efficiently bend the curves and go beyond sharp obstacles despite their non-topological origin. The unidirectional features disable back-scattering; however, weak surface-bulk interference prevails at the most obstructed paths. A gyro-odd-elastic wedge of different vertex angles and curvature radii has been discussed elsewhere (see Supplementary Note 5) to shed more light on the influence of the geometry.

Conclusions

In conclusion, we have investigated the elastodynamics in active media comprising both gyroscopic and odd-elastic effects. It is shown that such materials present highly unusual non-Hermitian

characteristics in that active systems may be driven to be stable or unstable due to the exchange of energy. More importantly, we showcase non-Hermitian Rayleigh waves that by the right choice of odd-elastic moduli travel along a strict unidirectional path, where the travel distance and degree of confinement, likewise can be tuned. Thanks to the resulting absence of reciprocity, such one-way gyro-odd-elastic waves, surprisingly display very strong robustness against uneven surfaces and sharp corners. Beyond the academic significance, we foresee that the unusual physics reported here can stimulate explorations in active devices, aiming at robust and scattering-immune guiding of surface acoustic waves. Fortunately, recent approaches have demonstrated viable routes towards gyroscopic and odd-elastic responses using robotics and piezoelectric metamaterials^{27,28,36–38}, which may pave the way for a gyro-odd elastodynamics implementation.

Methods

Based on an algorithm (see Supplementary Notes 2, 3), we have solved the modal solutions of Eq. (3) for both unbound and semi-infinite spaces as illustrated in Figs. 1–3. In addition, finite-element-based computations were implemented to simulate elastic waves propagating in active media using the PDE module of the commercial solver package COMSOL Multiphysics. When considering the eigenfrequency analysis of the slab in Fig. 4a, the vertical sides are subject to periodic boundary condition while the horizontal surfaces are set to be stress-free. In Fig. 4b, c, all boundaries are assumed to be stress-free.

Data availability

The data that support the plots within this paper and other findings of this study are available from the corresponding author upon reasonable request.

Code availability

The code for obtaining the results of this work are available from the corresponding author upon reasonable request.

Received: 7 February 2022; Accepted: 26 September 2022;

Published online: 13 October 2022

References

- Christensen, J., Kadic, M., Kraft, O. & Wegener, M. Vibrant times for mechanical metamaterials. *MRS Commun.* **5**, 453–462 (2015).
- Cosserat, E. & Cosserat, F. *Theorie des corps déformables* (A. Hermann et fils, 1909).
- Eringen, A. C. *Microcontinuum Field Theories: I. Foundations and Solids* (Springer Science & Business Media, 2012).
- Frenzel, T., Kadic, M. & Wegener, M. Three-dimensional mechanical metamaterials with a twist. *Science* **358**, 1072–1074 (2017).
- Milton, G. W. & Willis, J. R. On modifications of Newton's second law and linear continuum elastodynamics. *Proc. R. Soc. A* **463**, 855–880 (2007).
- Merkel, A., Romero-García, V., Groby, J.-P., Li, J. & Christensen, J. Unidirectional zero sonic reflection in passive \mathcal{PT} -symmetric Willis media. *Phys. Rev. B* **98**, 201102 (2018).
- Liu, Y. et al. Willis metamaterial on a structured beam. *Phys. Rev. X* **9**, 011040 (2019).
- Norris, A. N. Acoustic cloaking theory. *Proc. R. Soc. A* **464**, 2411–2434 (2008).
- Layman, C. N., Naify, C. J., Martin, T. P., Calvo, D. C. & Orris, G. J. Highly anisotropic elements for acoustic pentamode applications. *Phys. Rev. Lett.* **111**, 024302 (2013).
- Bückmann, T., Thiel, M., Kadic, M., Schittny, R. & Wegener, M. An elasto-mechanical unfeelability cloak made of pentamode metamaterials. *Nat. Commun.* **5**, 1–6 (2014).
- Miniaci, M., Pal, R. K., Morvan, B. & Ruzzene, M. Experimental observation of topologically protected helical edge modes in patterned elastic plates. *Phys. Rev. X* **8**, 031074 (2018).
- Rosendo López, M., Peñaranda, F., Christensen, J. & San-Jose, P. Flat bands in magic-angle vibrating plates. *Phys. Rev. Lett.* **125**, 214301 (2020).
- Gao, P. & Christensen, J. Topological vortices for sound and light. *Nat. Nanotechnol.* **16**, 487–489 (2021).

14. Wu, X. et al. Topological corner modes induced by dirac vortices in arbitrary geometry. *Phys. Rev. Lett.* **126**, 226802 (2021).
15. Wang, Y. et al. Observation of nonreciprocal wave propagation in a dynamic phononic lattice. *Phys. Rev. Lett.* **121**, 194301 (2018).
16. Shah, P. J. et al. Giant nonreciprocity of surface acoustic waves enabled by the magnetoelastic interaction. *Sci. Adv.* **6**, eabc5648 (2020).
17. White, D. L. Amplification of ultrasonic waves in piezoelectric semiconductors. *J. Appl. Phys.* **33**, 2547–2554 (1962).
18. Christensen, J., Willatzen, M., Velasco, V. R. & Lu, M.-H. Parity-time synthetic phononic media. *Phys. Rev. Lett.* **116**, 207601 (2016).
19. Gao, P., Willatzen, M. & Christensen, J. Anomalous topological edge states in non-hermitian piezophononic media. *Phys. Rev. Lett.* **125**, 206402 (2020).
20. Willatzen, M., Gao, P., Christensen, J. & Wang, Z. L. Acoustic gain in solids due to piezoelectricity, flexoelectricity, and electrostriction. *Adv. Funct. Mater.* **30**, 2003503 (2020).
21. Brun, M., Jones, I. S. & Movchan, A. B. Vortex-type elastic structured media and dynamic shielding. *Proc. R. Soc. A* **468**, 3027–3046 (2012).
22. Trainiti, G. et al. Time-periodic stiffness modulation in elastic metamaterials for selective wave filtering: theory and experiment. *Phys. Rev. Lett.* **122**, 124301 (2019).
23. McEvoy, M. A. & Correll, N. Materials that couple sensing, actuation, computation, and communication. *Science* **347**, 1261689 (2015).
24. Brandenbourger, M., Locsin, X., Lerner, E. & Coullais, C. Non-reciprocal robotic metamaterials. *Nat. Commun.* **10**, 1–8 (2019).
25. Wang, P., Lu, L. & Bertoldi, K. Topological phononic crystals with one-way elastic edge waves. *Phys. Rev. Lett.* **115**, 104302 (2015).
26. Nash, L. M. et al. Topological mechanics of gyroscopic metamaterials. *Proc. Natl. Acad. Sci. USA* **112**, 14495–14500 (2015).
27. Zhao, Y., Zhou, X. & Huang, G. Non-reciprocal rayleigh waves in elastic gyroscopic medium. *J. Mech. Phys. Solids* **143**, 104065 (2020).
28. Carta, G., Colquitt, D., Movchan, A., Movchan, N. & Jones, I. Chiral flexural waves in structured plates: directional localisation and control. *J. Mech. Phys. Solids* **137**, 103866 (2020).
29. Betti, E. Teoria della elasticita. *Il Nuovo Cimento (1869-1876)* **7**, 158–180 (1872).
30. Scheibner, C. et al. Odd elasticity. *Nat. Phys.* **16**, 475–480 (2020).
31. Marijanović, F., Moroz, S. & Jeevanesan, B. Rayleigh waves and cyclotron surface modes of gyroscopic metamaterials. *Phys. Rev. B* **106**, 024308 (2022).
32. Scheibner, C., Irvine, W. T. M. & Vitelli, V. Non-hermitian band topology and skin modes in active elastic media. *Phys. Rev. Lett.* **125**, 118001 (2020).
33. Fodor, E. & Souslov, A. Optimal power and efficiency of odd engines. *Phys. Rev. E* **104**, L062602 (2021).
34. Torres, L. E. F. F. Perspective on topological states of non-hermitian lattices. *J. Phys. Mater.* **3**, 014002 (2019).
35. Souslov, A., Dasbiswas, K., Fruchart, M., Vaikuntanathan, S. & Vitelli, V. Topological waves in fluids with odd viscosity. *Phys. Rev. Lett.* **122**, 128001 (2019).
36. Chen, Y., Li, X., Scheibner, C., Vitelli, V. & Huang, G. Realization of active metamaterials with odd micropolar elasticity. *Nat. Commun.* **12**, 1–12 (2021).
37. Cheng, W. & Hu, G. Odd elasticity realized by piezoelectric material with linear feedback. *Sci. China Phys. Mech.* **64**, 1–10 (2021).
38. Brandenbourger, M., Scheibner, C., Veenstra, J., Vitelli, V. & Coullais, C. Limit cycles turn active matter into robots. Preprint at <https://arxiv.org/abs/2108.08837> (2021).

Acknowledgements

J.C. acknowledges the support from the European Research Council (ERC) through the Starting Grant No. 714577 PHONOMETEA and from the MINECO through a Ramón y Cajal grant (Grant No. RYC-2015-17156). Y.Q. acknowledges the support from the National Natural Science Foundation of China (Grant Nos. U2141244, 11922208, 11932011, 12121002) and the Oceanic Interdisciplinary Program of Shanghai Jiao Tong University (Grant No. SL2021ZD104). P.G. acknowledges the support from the National Natural Science Foundation of China (Grant No. 12202267), Shanghai Pujiang Program (Grant No. 22PJ1405300) and the Starting Grant of Shanghai Jiao Tong University (Grant No. WH220402014).

Author contributions

P.G. and J.C. conceived the project. P.G. conducted and carried out the numerical simulations. J.C. and Y.Q. supervised the project. All authors contributed to the discussions of the results and the manuscript preparation.

Competing interests

The authors declare no competing interests. Johan Christensen is a Guest Editor for Communications Materials and was not involved in the editorial review of, or the decision to publish, this Article.

Additional information

Supplementary information The online version contains supplementary material available at <https://doi.org/10.1038/s43246-022-00297-5>.

Correspondence and requests for materials should be addressed to Yegao Qu or Johan Christensen.

Peer review information Communications Materials thanks Emanuele Riva and the other, anonymous, reviewer(s) for their contribution to the peer review of this work. Primary Handling Editor: Aldo Isidori

Reprints and permission information is available at <http://www.nature.com/reprints>

Publisher's note Springer Nature remains neutral with regard to jurisdictional claims in published maps and institutional affiliations.



Open Access This article is licensed under a Creative Commons Attribution 4.0 International License, which permits use, sharing, adaptation, distribution and reproduction in any medium or format, as long as you give appropriate credit to the original author(s) and the source, provide a link to the Creative Commons license, and indicate if changes were made. The images or other third party material in this article are included in the article's Creative Commons license, unless indicated otherwise in a credit line to the material. If material is not included in the article's Creative Commons license and your intended use is not permitted by statutory regulation or exceeds the permitted use, you will need to obtain permission directly from the copyright holder. To view a copy of this license, visit <http://creativecommons.org/licenses/by/4.0/>.

© The Author(s) 2022